

# A Density Functional Study of the Dimerization of Phosphaalkynes in the Presence of Transition Metal Fragments

Steven Creve,<sup>[a]</sup> Minh Tho Nguyen,<sup>\*[a]</sup> and Luc G. Vanquickenborne<sup>[a]</sup>

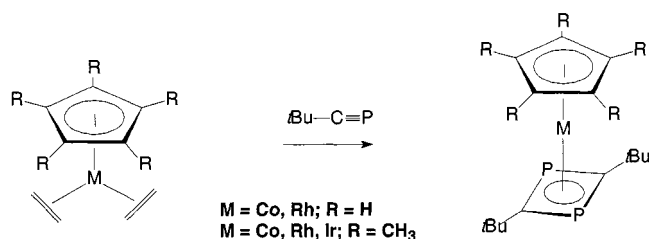
**Keywords:** Phosphaalkynes / Dimerization mechanism / Diphosphacyclobutenes / Density functional theory / Ab initio calculations

The dimerization of phosphaalkynes ( $R-C\equiv P$ ,  $R = H, Me, tBu$ ) without and with the presence of transition metal fragments, including CpCo (Cp = cyclopentadienyl) and COT-Ti (COT = cyclooctatetraene), has been probed using density functional theory calculations (B3LYP with different basis sets). MP2 and CCSD(T) calculations were also performed for the

$[H_2C_2P_2]$  systems. In an attempt to address the exciting controversy and uncertainty about phosphaalkyne dimerization, a number of dimer formation mechanisms proposed in the literature have been examined. Some new and plausible intermediates have also been identified.

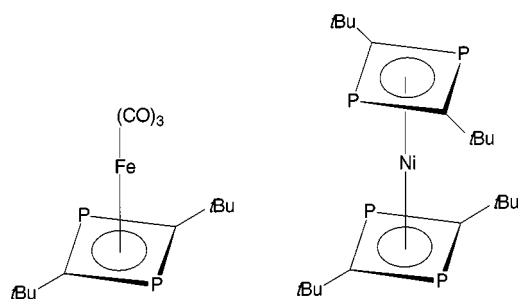
## 1. Introduction

In 1986, two independent groups<sup>[1][2]</sup> first reported the cyclodimerization of a phosphaalkyne ( $R-C\equiv P$ ) in the coordination sphere of cobalt, rhodium, and iridium centers, yielding a 1,3-diphosphacyclobutadiene ring (referred to hereafter as 1,3-DPCB), as shown in Scheme 1.



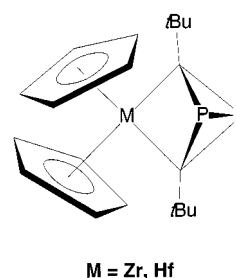
Scheme 1. Formation of 1,3-DPCB in metal complexes

Soon afterwards, other similar complexes containing iron were discovered,<sup>[3][4]</sup> as well as a sandwich complex of nickel containing two 1,3-DPCB rings<sup>[5]</sup> (Scheme 2).



Scheme 2. Observation of 1,3-DPCB in Fe and Ni complexes

With Zr or Hf as metallic center, however, a 1,3-diphosphabicyclo[1.1.0]butanediyl ligand was shown to be formed<sup>[6][7]</sup> (Scheme 3).



Scheme 3. Observation of bicyclic dimers in Zr, Hf complexes

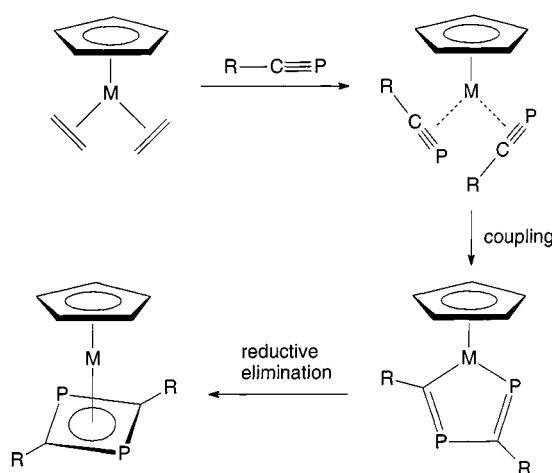
Interestingly, it has been proven extremely difficult, if not impossible, to displace the  $\eta^4$ -ligated  $P_2C_2tBu_2$  rings from any of these complexes, which is in clear contrast to the behavior of analogous cyclobutadiene rings.

As far as the formation of the 1,3-DPCB complexes is concerned (Scheme 4), it has been assumed that first a bis( $\pi$ -phosphaalkyne) complex is formed, followed by a coupling process to give a 1-metalla-2,4-diphosphacyclopentadienyl complex. The latter can then undergo a reductive elimination yielding the product 1,3-DPCB complex. This mechanism was postulated by analogy to the reaction sequence taking place when cyclobutadiene complexes are formed out of alkynes.<sup>[8][9]</sup>

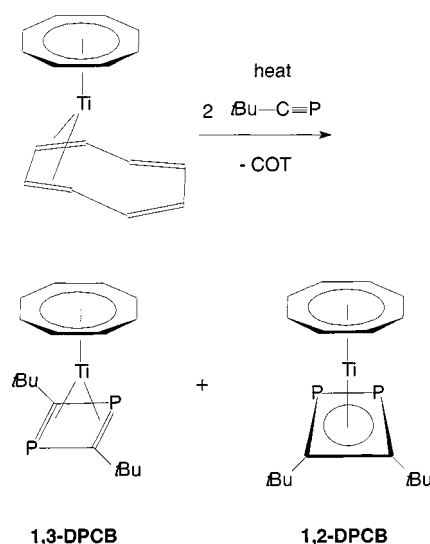
Further evidence for this reaction mechanism was provided by Binger et al. who found the existence of a 1,4-diphospha-2-rhodacyclopentadiene species as intermediate in the formation of the 1,3-DPCB complex<sup>[10]</sup> (Scheme 5). These authors were able to characterize the 1,4-diphospha-2-rhodacyclopentadiene species by X-ray diffraction studies.

However, no clear-cut evidence has been found yet proving or disproving that the mechanisms of formation of other complexes (such as shown in Schemes 1 and 2) also proceed via 1-metalla-2,4-diphosphacyclopentadienyl inter-

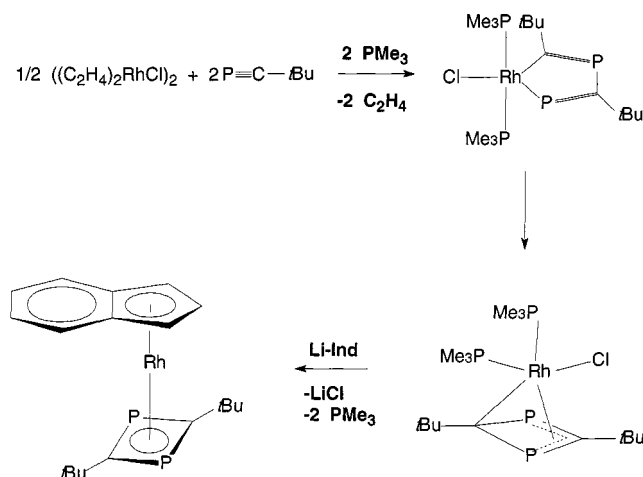
<sup>[a]</sup> Department of Chemistry, University of Leuven, Celestijnenlaan 200F, B-3001 Leuven, Belgium



Scheme 4. Proposed formation mechanism of 1,3-DPCB involving metallacyclobutadiene intermediate



Scheme 6. Formation of both 1,3- and 1,2-DPCB when Ti complexes were used



Scheme 5. Proposed formation mechanism of 1,3-DPCB in Rh complexes

mediates. Another interesting point is that, when using Co or Rh as metallic center, a 1,2-diphosphacyclobutadiene complex has never been detected (referred to hereafter as 1,2-DPCB). In fact, the first example of a 1,2-DPCB complex has only recently been characterized by making use of titanium<sup>[11][12]</sup> (Scheme 6).

In the case of Ti, both the 1,3-DPCB and 1,2-DPCB complexes have been found. While the latter has a large delocalization of electrons within the ring, the former shows two short and two long P–C bonds. Again, this is in contrast to the 1,3-DPCB complexes of Co and Rh, where the carbon-phosphorus ring is also largely delocalized. Without the presence of metal compounds, a cyclotetramerization of phosphalkynes has been found upon heating, which leads to a tetraphosphacubane.<sup>[13]</sup> Formation of the latter has been postulated to involve a 1,3-DPCB intermediate.

In our previous work,<sup>[14]</sup> different equilibrium and transition structures on the  $[C_2H_2P_2]$  potential energy surface have been calculated. It turned out that 1,2-DPCB tends to be more stable than the 1,3-DPCB by about 30–40 kJ/mol.

Moreover, the activation energy for 1,2-DPCB formation in a head-to-head approach is also smaller.

All facts considered, a number of intriguing questions remain unanswered:

- Why is, in the case of Co and Rh, only the 1,3-DPCB complex found, and not the 1,2-DPCB, although the latter is more stable in free form, as found in previous work?<sup>[14]</sup>
- Concerning the free DPCB species, what is the influence of bulkier substituents on the carbon atoms, i.e. how large are steric effects in these systems? As a matter of fact, the available experiments have usually been carried out with phosphalkynes  $R-C\equiv P$  where  $R = tBu$  or other sterically hindered substituents.

• With Ti as metallic center, both 1,2-DPCB and 1,3-DPCB complexes are found. Remarkably, however, the 1,3-DPCB complex shows two different P–C bond lengths, in contrast to the Co and Rh cases, where a more delocalized DPCB ring is obtained.

• Finally, is the mechanism via metallacyclobutadiene intermediates indeed a valid reaction scheme?

In an attempt to obtain more insight into this interesting area of low-coordinated phosphorus chemistry, a computational study has been carried out on free DPCB species on the one hand ( $R_2C_2P_2$ , with  $R = H, CH_3$ , and  $tBu$ ), and some representative metal complexes on the other hand [ $Cp-Co-(R_2C_2P_2)$ , with  $R = H, CH_3$ , and  $Cp =$  cyclopentadienyl;  $COT-Ti-(H_2C_2P_2)$  with  $COT =$  cyclooctatetraene].

## 2. Computational Details

The species considered include the important  $[R_2C_2P_2]$  isomers with  $R = H, CH_3$ , and  $tBu$ ,  $[Cp-Co-(R_2C_2P_2)]$  isomers ( $R = H, CH_3$ ;  $Cp =$  cyclopentadienyl), and a number of  $COT-Ti-[H_2C_2P_2]$  isomers ( $COT =$  cyclooctatetraene).

ene). For the sake of comparison, we also calculated some isomers of  $\text{Cp-Co-[H}_4\text{C}_4\text{]}$ .

All geometries have been optimized using the B3LYP density functional<sup>[15][16]</sup> with the 6-31G(d,p) basis set. For the metal elements, a (14s,9p,5d)/[8s,5p,3d] basis set was used,<sup>[17]</sup> augmented by two p functions,<sup>[18]</sup> one d function,<sup>[19]</sup> and one f function. For the free species ( $\text{R}_2\text{C}_2\text{P}_2$ ) with  $\text{R} = \text{H}$  and  $\text{CH}_3$ , harmonic vibrational analyses have been performed as well at the B3LYP/6-31G(d,p) level. MP2 geometry optimizations using the 6-31G(d,p) basis set have been performed for the  $[\text{H}_2\text{C}_2\text{P}_2]$  compounds, including vibrational analysis. To obtain improved relative energies, coupled cluster CCSD(T)/6-311+G (2df,p) single-point calculations using the MP2-optimized geometries as well as B3LYP/6-311+G(2df,p) single-point calculations have also been carried out for the  $[\text{H}_2\text{C}_2\text{P}_2]$  isomers.

While the Gaussian 98 electronic structure program<sup>[20]</sup> was used for calculating the uncomplexed species, the Mulliken software<sup>[21]</sup> was used for calculations on complexed species. Both the geometry optimizations in Gaussian 98 and in the Mulliken software were performed with a convergence criterion of  $4.5 \cdot 10^{-4}$  Hartree/Bohr for the gradients.

### 3. Results and Discussion

#### 3.1 Uncomplexed Dimerization Products

Figure 1 shows schematic representations of the uncomplexed species considered in this work, along with the labeling conventions used throughout. Tables 1 and 2 contain the optimized geometrical parameters and relative energies, respectively. The minima considered include the free phosphoalkynes **1a–c**, the two valence isomers of 1,2-DPCB **2a–c** and **3a–c**, and 1,3-DPCB **4a–c**. While **1a/2a** and **1b/2b** are transition states for the so-called "head-to-head" cycloaddition of two RCP molecules leading to 1,2-DPCB, **1a/4a** and **1b/4b** describe the "head-to-tail" reaction yielding 1,3-DPCB. In the following paragraphs, mentioned geometrical parameters refer to the B3LYP-optimized values, unless otherwise noted.

##### 3.1.1 Dimerization of the Parent $\text{H-C}\equiv\text{P}$

Concerning the dimerization products of HCP, it is seen from Table 2 that these products are all bound with respect to the free phosphoalkynes. This fact is reproduced at all levels of theory, including B3LYP, MP2, and CCSD(T), with one exception, being **4a** at the MP2 level.

Both valence isomers **2a** and **3a** of the head-to-head dimers exist. While **2a** clearly shows a  $\text{C}=\text{C}$  bond (1.330 Å) and a  $\text{P}=\text{P}$  bond (2.071 Å), the reverse is seen for **3a**, having single  $\text{C}-\text{C}$  and  $\text{P}-\text{P}$  bonds (1.463 and 2.488 Å, respectively) and double  $\text{C}=\text{P}$  bonds (1.698 Å). Both **2a** and **3a** possess a trapezoid structure. Of the two valence isomers, **2a** with  $\text{C}=\text{C}$  and  $\text{P}=\text{P}$   $\pi$  bonds is the most stable, lying 11 kJ/mol below **3a** at the B3LYP level and 12 kJ/mol at the CCSD(T) level.

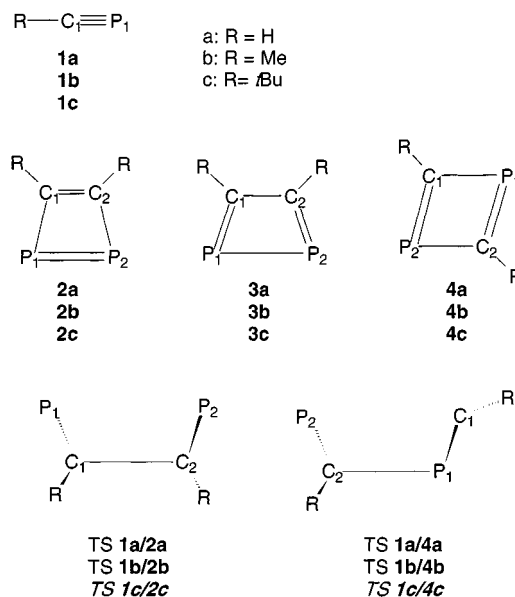


Figure 1. Schematic representations of noncomplexed species considered, along with the labeling conventions; labels in *italics* refer to species mentioned in the text, but not actually computed in this work

Table 1. B3LYP/6-31G(d,p)-optimized bond lengths [Å] and angles [°] for the differently substituted uncomplexed diphosphacyclobutadienes under consideration; values in parentheses refer to MP2/6-31G(d,p)-optimized parameters (see Figure 1 for definition of structures and atom labels)

	$\text{C}_1\text{P}_1$		$\text{RC}_1$			
<b>1a</b>	1.543	(1.561)	1.074	(1.070)		
<b>1b</b>	1.550		1.460			
<b>1c</b>	1.552		1.473			
	$\text{C}_1\text{P}_1$	$\text{C}_1\text{C}_2$	$\text{P}_1\text{P}_2$	$\text{C}_1\text{C}_2\text{P}_2$	$\text{P}_1\text{P}_2\text{C}_2$	$\text{RC}_1\text{C}_2$
<b>2a</b>	1.924	1.330	2.071	101.1	78.9	129.7
	(1.900)	(1.339)	(2.081)	(101.3)	(78.7)	(129.5)
<b>2b</b>	1.926	1.339	2.067	100.9	79.1	132.3
<b>2c</b>	1.942	1.351	2.053	100.4	79.5	137.3
<b>3a</b>	1.698	1.463	2.488	107.6	72.4	125.0
	(1.702)	(1.460)	(2.455)	(107.0)	(73.0)	(125.7)
<b>3b</b>	1.703	1.488	2.447	106.4	73.6	124.5
<b>3c</b>	1.708	1.533	2.371	104.1	75.8	133.0
	$\text{C}_1\text{P}_1$	$\text{C}_1\text{P}_2$	$\text{RC}_1$	$\text{C}_1\text{P}_1\text{C}_2$	$\text{P}_1\text{C}_2\text{P}_2$	
<b>4a</b>	1.925	1.679	1.086	81.1	98.9	
	(1.897)	(1.682)	(1.080)	(81.4)	(98.6)	
<b>4b</b>	1.931	1.692	1.482	80.6	99.4	
<b>4c</b>	1.934	1.694	1.499	80.7	99.3	
	$\text{C}_1\text{C}_2$	$\text{P}_1\text{P}_2$	$\text{C}_1\text{P}_1$	$\text{P}_1\text{C}_1\text{C}_2$	$\text{P}_1\text{C}_1\text{P}_2$	$\text{P}_1\text{C}_1\text{C}_2\text{P}_2$
<b>1a/2a</b>	1.908	4.068	1.593	117.3	143.5	107.2
	(1.868)	(4.200)	(1.608)	(120.2)	(140.6)	(114.9)
<b>1b/2b</b>	1.885	4.000	1.608	112.1	141.6	116.6
	$\text{C}_1\text{P}_2$	$\text{C}_2\text{P}_1$	$\text{C}_1\text{P}_1$	$\text{C}_2\text{P}_2$	$\text{C}_1\text{P}_1\text{C}_2$	$\text{C}_1\text{P}_1\text{C}_2\text{P}_2$
<b>1a/4a</b>	3.051	1.960	1.720	1.607	102.2	74.3
	(3.015)	(2.045)	(1.674)	(1.596)	(99.8)	(75.4)
<b>1b/4b</b>	3.234	1.996	1.713	1.613	99.2	91.2

The head-to-tail dimer **4a** has a parallelogram structure, with clearly distinguishable alternating single  $\text{C}-\text{P}$  and double  $\text{C}=\text{P}$  bonds (1.925 and 1.679 Å, respectively). The  $\text{C}-\text{P}-\text{C}$  angles turn out to be somewhat smaller than  $90^\circ$  (81.10); consequently, the  $\text{P}-\text{C}-\text{P}$  angles are larger than  $90^\circ$  (98.9°). **4a** turns out to be the least stable of the isomers considered here. Although it is bound by more than 20 kJ/mol with respect to the free phosphoalkyne at the B3LYP

Table 2. Relative energies [kJ/mol] of uncomplexed species considered

	B3LYP <sup>a</sup> 6-31G(d,p)	MP2 <sup>b</sup>	B3LYP <sup>a</sup> 6-311+G(2df,p)	CCSD(T) <sup>b</sup>
<b>1a</b>	0.0	0.0	0.0	0.0
<b>2a</b>	-74.4	-21.4	-69.3	-66.3
<b>3a</b>	-68.1	-14.3	-58.8	-54.3
<b>4a</b>	-21.1	15.3	-21.2	-23.8
<b>TS 1a/2a</b>	107.5	105.8	98.2	100.2
<b>TS 1a/4a</b>	177.0	258.1	164.9	185.0

	B3LYP <sup>a</sup> 6-31G(d,p)	B3LYP <sup>c</sup> 6-31G(d,p)
<b>1b</b>	0.0	<b>1c</b> 0.0
<b>2b</b>	-46.3	<b>2c</b> -5.7
<b>3b</b>	-36.7	<b>3c</b> 9.8
<b>4b</b>	2.0	<b>4c</b> -3.1
<b>TS 1b/2b</b>	129.5	
<b>TS 1b/4b</b>	203.5	

[a] Based on B3LYP geometries and including ZPE(B3LYP). – [b] Based on MP2 geometries and including ZPE(MP2). – [c] Based on B3LYP geometries and without ZPE.

and CCSD(T) levels, MP2 predicts it to be less stable than the separated monomers.

For the dimerization reaction, two transition states have been located. While TS **1a/2a** connects the free HCP molecules to the 1,2-DPCB having C=C and P=P  $\pi$  bonds, TS **1a/4a** represents the transition structure for head-to-tail dimerization. At the B3LYP level, the head-to-head process has an energy barrier of 98 kJ/mol, and the head-to-tail reaction passes over a 165 kJ/mol energy barrier. While MP2 is in good agreement with B3LYP and CCSD(T) concerning the former process, the MP2 head-to-tail energy barrier is considerably overestimated with respect to the B3LYP or CCSD(T) values. Most likely, this is due to the fact that MP2 is not able to treat nondynamical correlation energy, whereas the DFT and CCSD(T) can do so to some extent (vide infra). Qualitatively, however, all levels of theory confirm that the head-to-head product **2a** is both kinetically and thermodynamically favored over its head-to-tail counterpart.

In agreement with results of previous work,<sup>[14]</sup> the two HCP monomers approach each other in nearly perpendicular planes to form the 1,2- and 1,3-DPCB (TS **1a/2a** and **1a/4a**). In TS **1a/2a**, formation of the CP bond has clearly progressed further than the PP bond ( $C_1C_2 = 1.908$  Å, in contrast to  $P_1P_2 = 4.068$  Å). The same behavior is seen in TS **1a/4a**, where one forming CP bond is markedly shorter than the other ( $C_2P_1 = 1.960$  Å versus  $C_1P_2 = 3.051$  Å). Both transition structures thus imply a highly asynchronous formation of the two new chemical bonds. This suggests a radical mechanism for this symmetry-forbidden [2+2] cycloaddition.

In general, no severe geometrical differences between the MP2- and B3LYP-optimized structures are found. Concerning relative energies, however, a close examination of Table 2 shows that, while B3LYP yields results in excellent agreement with the CCSD(T) values, MP2 is often in considerable error with the CCSD(T) level.

It has to be noted, finally, that a proper description of the dimerization process of R–C≡P species requires a treatment using a multi-configurational wavefunction (MCSCF).

However, such a treatment is beyond the scope of the present work. Note also that density functional methods are generally believed to incorporate at least some part of the nondynamical correlation. Therefore, in view of the good agreement between our B3LYP and CCSD(T) calculations, we think that the present calculations provide a sufficiently accurate basis for drawing the conclusions described above.

### 3.1.2 Dimerization of Me–C≡P and *t*Bu–C≡P

In an attempt to tackle the question posed in the introduction concerning the influence of bulkier substituents on C, B3LYP calculations have been carried out for the heavier phosphalkynes MeCP and *t*BuCP. Due to limitations in computational resources, harmonic frequency calculations have not been carried out for the latter, and TS **1c/2c** and **1c/4c** have not been calculated.

Substitution of H in the parent phosphalkyne by CH<sub>3</sub> yields the following relative energy ordering for the dimers: **2b** < **3b** < **4b**, in analogy with the parent species. However, the stability with respect to the free phosphalkynes is considerably changed upon Me substitution. The 1,3-DPCB **4b** lies now even higher in energy than the monomers. The reason for this alteration of relative stabilities has probably to be found in the stabilization of the monomers by larger alkyl substituents. The energy difference between **2b** and **4b** amounts to 48 kJ/mol, and has thus been decreased with respect to the unsubstituted case (53 kJ/mol). This fact possibly points to a slight destabilization of the 1,2-DPCB **2b** due to steric interactions between the two methyl groups. Another indication for steric repulsion between the methyl groups is found in the RC<sub>1</sub>C<sub>2</sub> angle of **2b** which is 2.6° larger than the corresponding value for **2a**. The transition structures for head-to-head and head-to-tail cycloaddition reactions are found at 130 kJ/mol and 204 kJ/mol, respectively, relative to the monomers. As a consequence, the energy barriers have been increased with respect to the HCP case (due to stabilization of the MeCP monomers), whereas the relative ordering of the two TSs has remained nearly constant. Proceeding in the opposite direction, both DPCBs become less stable with regard to cycloreversion.

Replacing the hydrogen atom by the sterically demanding *t*Bu groups has considerable consequences on the relative stabilities. Only the 1,2-DPCB **2c** and 1,3-DPCB **4c** are stabilized with respect to the free monomers. The corresponding stabilization energies, however, amount to only 6 and 3 kJ/mol, respectively. It thus seems that replacing Me by *t*Bu further stabilizes the monomers. The energy gap between the two valence isomers **2c** and **3c** has further increased to 16 kJ/mol, whereas it was 6 kJ/mol for **2a-3a** and 10 kJ/mol for **2b-3b**. Most remarkable is the fact that the energy difference between the head-to-head adduct **2c** and



the head-to-tail dimer **4c** has decreased to only 3 kJ/mol, in favor of the former. This points to a considerable destabilization of **2c** by steric hindrance of the *t*Bu groups. Again, this observation is in agreement with an  $\text{RC}_1\text{C}_2$  angle of  $137.3^\circ$  in **2c**, as compared with that of  $129.7^\circ$  for **2a**.

### 3.2 Metal Complexes of the $\text{R}-\text{C}\equiv\text{P}$ Dimers

Overviewing the results gathered from calculations on the free  $\text{R}-\text{C}\equiv\text{P}$  dimers, it turns out that in all cases considered, the 1,2-DPCB dimer is the more stable. Therefore, it is most intriguing why, in the presence of transition metal fragments of Co, Rh, Ir, Fe, and Ni (see Schemes 1 and 2), only the 1,3-DPCB complexes are found. Interestingly, when Ti is used, both dimers are found (see Scheme 6). We have therefore carried out calculations on the model compounds shown in Figure 2. Two transition metal fragments have been considered: the  $14e^-$  CpCo fragment (Cp cyclopentadiene) and the  $12e^-$  COT-Ti fragment (COT = cyclooctatetraene). The calculations include full B3LYP geometry optimizations and energy calculations. The basis sets used are specified in a previous section. Optimized geometrical parameters and relative energies of the complexes considered are shown in Tables 3 and 4, respectively.

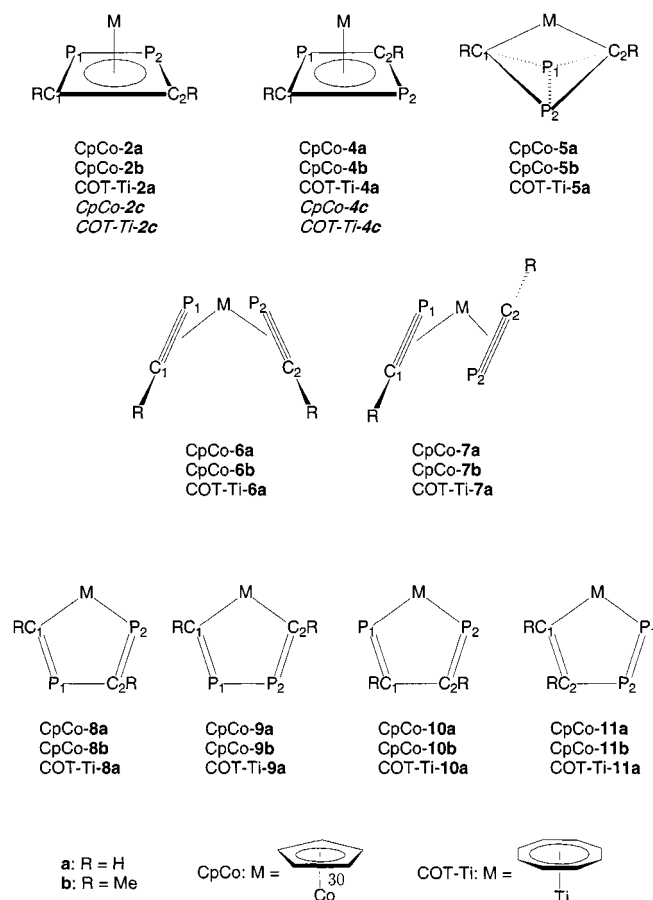


Figure 2. Schematic representations of the complexes considered, along with the labeling conventions; labels in *italics* refer to species mentioned in the text, but not actually computed in this work

Table 3. B3LYP/6-31G(d,p)-optimized bond lengths [ $\text{\AA}$ ] and angles [ $^\circ$ ] for the various complexed species under consideration (see Figure 2 for definition of structures and atom labels)

	MP <sub>1</sub>	MC <sub>1</sub>	C <sub>1</sub> P <sub>1</sub>	C <sub>1</sub> C <sub>2</sub>	P <sub>1</sub> P <sub>2</sub>	C <sub>1</sub> P <sub>1</sub> P <sub>2</sub>	C <sub>1</sub> C <sub>2</sub> P <sub>2</sub>
CpCo-2a	2.293	2.037	1.812	1.416	2.238	76.9	103.1
CpCo-2b	2.286	2.052	1.820	1.423	2.230	77.2	102.8
COT-Ti-2a	2.523	2.313	1.811	1.404	2.232	76.8	103.2
exp. <sup>a</sup>	2.491	2.387	1.811	-	2.175	78.1	101.9
	MP <sub>1</sub>	MC <sub>1</sub>	C <sub>1</sub> P <sub>1</sub>	C <sub>1</sub> P <sub>2</sub>	C <sub>1</sub> P <sub>1</sub> C <sub>2</sub>	P <sub>1</sub> C <sub>1</sub> P <sub>2</sub>	C <sub>1</sub> P <sub>1</sub> P <sub>2</sub> C <sub>2</sub>
CpCo-4a	2.267	2.050	1.801	1.801	79.6	100.0	169.3
CpCo-4b	2.267	2.048	1.808	1.809	80.3	99.2	168.7
exp. <sup>b</sup>	2.243	2.058	1.797	1.797	80.9	98.9	172.0
COT-Ti-4a	2.530	2.302	1.795	1.795	80.1	99.3	167.6
exp. <sup>c</sup>	2.5180	2.333	1.747	1.836	81.8	97.8	-
	MP <sub>1</sub>	MC <sub>1</sub>	C <sub>1</sub> P <sub>1</sub>	P <sub>1</sub> P <sub>2</sub>		C <sub>1</sub> P <sub>1</sub> P <sub>2</sub> C <sub>2</sub>	
CpCo-5a	2.822	1.897	1.904	2.126		92.1	
CpCo-5b	2.807	1.900	1.911	2.133		93.4	
exp. <sup>d</sup>	-	-	1.900	2.147		70	
COT-Ti-5a	2.985	2.087	1.895	2.146		95.6	
	MC <sub>1</sub>	MP <sub>2</sub>	C <sub>1</sub> P <sub>1</sub>	P <sub>1</sub> C <sub>2</sub>	C <sub>2</sub> P <sub>2</sub>		
CpCo-8a	1.778	2.267	1.717	1.808	1.684		
CpCo-8b	1.776	2.276	1.736	1.818	1.685		
COT-Ti-8a	2.096	2.593	1.682	1.841	1.687		
	MC <sub>1</sub>	C <sub>1</sub> P <sub>1</sub>	P <sub>1</sub> P <sub>2</sub>				
CpCo-9a	1.844	1.671	2.309				
CpCo-9b	1.876	1.682	2.271				
COT-Ti-9a	2.122	1.680	2.299				
	MP <sub>1</sub>	P <sub>1</sub> C <sub>1</sub>	C <sub>1</sub> C <sub>2</sub>				
CpCo-10a	2.230	1.707	1.435				
CpCo-10b	2.221	1.718	1.453				
COT-Ti-10a	2.560	1.703	1.452				
	MC <sub>1</sub>	MP <sub>1</sub>	C <sub>1</sub> C <sub>2</sub>	C <sub>2</sub> P <sub>2</sub>	P <sub>1</sub> P <sub>2</sub>		
CpCo-11a	1.857	2.182	1.341	1.828	2.067		
CpCo-11b	1.882	2.186	1.351	1.828	2.055		

[a] Experimental parameters for the *t*Bu analog COT-Ti-2c, ref.<sup>[11]</sup> – [b] Experimental parameters for the *t*Bu analog CpCo-4c, ref.<sup>[22]</sup> – [c] Experimental parameters for the *t*Bu analog COT-Ti-4c, ref.<sup>[11]</sup> – [d] Experimental parameters for the Cp<sub>2</sub>Zr complex of the 2,4-di-*tert*-butyl-1,3-diphosphabicyclo[1.1.0]butanediyl ligand, ref.<sup>[6]</sup>

Table 4. Relative energies [kJ/mol] of the complexes considered

	B3LYP	B3LYP	B3LYP
CpCo-2a	0.0	CpCo-2b	0.0
CpCo-4a	45.9	CpCo-4b	52.3
CpCo-5a	256.2	CpCo-5b	269.4
CpCo-6a	247.2	CpCo-6b	227.5
CpCo-7a	245.3	CpCo-7b	220.4
CpCo-8a	347.9	CpCo-8b	359.0
CpCo-9a	349.0	CpCo-9b	372.0
CpCo-10a	326.1	CpCo-10b	349.3
CpCo-11a	308.3	CpCo-11b	319.9
CpCo-12a	181.4	CpCo-12b	190.4
		COT-Ti-2a	0.0
		COT-Ti-4a	53.8
		COT-Ti-5a	173.9
		COT-Ti-6a	272.5
		COT-Ti-7a	277.2
		COT-Ti-8a	229.6
		COT-Ti-9a	248.5
		COT-Ti-10a	183.7
		COT-Ti-11a	-
		COT-Ti-12a	162.7
	B3LYP		
A	0.0		
B	236.5		
C	173.3		
D	354.3		

#### 3.2.1 Cobalt Complexes of $\text{H}-\text{C}\equiv\text{P}$ Dimers

While the uncomplexed 1,2-DPCB and 1,3-DPCB clearly show alternating single and double bonds, their complexed counterparts CpCo-2a and CpCo-4a have bond lengths between single and double [ $r(\text{CC}) \approx 1.41 \text{ \AA}$ ,  $r(\text{CP}) \approx 1.81 \text{ \AA}$ , and  $r(\text{PP}) \approx 2.23 \text{ \AA}$ ]. Complexation of the dimers thus yields a shortening of the single bonds and a lengthening of the double bonds. This is a geometrical indication that the DPCB rings become less antiaromatic if complexed to

a CpCo fragment. Another indication of this behavior is the fact that complexation of **4a**, which has a parallelogram structure, leads to CpCo-**4a** where the diphosphacyclobutadiene unit exhibits a rhombic structure with four equal CP bond lengths.

Concerning the relative stabilities of both CpCo-**2a** and CpCo-**4a**, it seems that complexation has not much altered the situation with respect to the free dimers. While in free form, 1,2-DPCB lies 53 kJ/mol below 1,3-DPCB (B3LYP), in complexed form this energy gap is slightly decreased to 46 kJ/mol. Experimentally observed complexes of CpCo, however, are formed of *t*BuCP instead of HCP. In the previous section, it was calculated that the **2a** – **4a** energy gap decreases from 53 kJ/mol to 3 kJ/mol for **2c** – **4c**. By transferring this energy effect to the CpCo-**2a** – CpCo-**4a** energy difference, one can estimate the energy gap between CpCo-**2c** and CpCo-**4c** to be –5 kJ/mol, in favor of the latter. Even if such a crude approximation would be correct, the energy difference is too small and as such it could not explain why exclusively CpCo-**4a** complexes are found experimentally, and not the CpCo-**2a** complexes. Therefore, it seems necessary to take a closer look at the way the DPCB complexes are formed.

It has been proposed in the literature,<sup>[6][22]</sup> that the formation of diphosphacyclobutadiene complexes proceeds by the reaction sequence shown in Scheme 4, in analogy with that of cyclobutadiene complexes resulting from bis( $\pi$ -acetylene) complexes.<sup>[8][9]</sup> Therefore, a number of additional structures have also been calculated. These include the bis( $\pi$ -phosphaalkyne) complexes CpCo-**6a** and CpCo-**7a**, and four possible cobalt species CpCo-**8a**–CpCo-**11a**. For the sake of comparison, the all-carbon analogues, shown in Figure 3, have been computed as well. For the latter molecules, Table 4 shows that the bis( $\pi$ -acetylene) complex **B** lies higher in energy than the CpCoCb complex **A** by 237 kJ/mol. The cobalt complex **C** is found at an intermediate position of 173 kJ/mol. Hence, the **B** → **C** → **A** reaction seems possible for these species, and it has indeed been found experimentally.<sup>[8][9]</sup> A different situation appears when the acetylene molecules are replaced by H–C≡P species. Two bis( $\pi$ -phosphaacetylene) complexes are possible, CpCo-**6a** and CpCo-**7a**. While in the former complex, the two HCP molecules are side-on coordinated in a head-to-head fashion, the latter complex has them oriented in a head-to-tail manner. The complexes are found at 247 and 245 kJ/mol above CpCo-**2a**, respectively, which is very similar to the situation of **A** and **B**. However, the cobalt complexes CpCo-**8a**, CpCo-**9a**, CpCo-**10a**, and CpCo-**11a** are found at a much higher relative energy than the bis( $\pi$ -phosphaacetylene) complexes. Note that CpCo-**11a** has been calculated only for the sake of completeness, since it seems not possible that CpCo-**11a** can be formed starting from CpCo-**6a** or CpCo-**7a**. The relative energies of these cobalt complexes range from 308 to 349 kJ/mol, with respect to CpCo-**2a**. Hence, it is unlikely that these species intervene as intermediates, such as shown in Scheme 4. In this respect, it is noteworthy that direct fragmentation of a complexed cyclobutadiene ligand into two acetylene ligands, without prior

formation of a cobaltacyclopentadiene intermediate, has been observed.<sup>[23]</sup> This result suggests that the reverse – direct formation of cyclobutadiene out of two acetylene ligands – is also possible. Since the cobalt intermediates appear to be too high in relative energy in the case of diphosphacyclobutadiene complexes, it is tempting to say that a direct reaction of CpCo-**6a** or CpCo-**7a** to CpCo-**2a** or CpCo-**4a** might be possible.

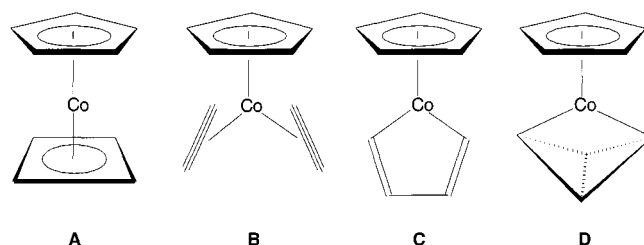


Figure 3. Schematic representations of the all-carbon complexes considered, along with the labeling conventions

Since Zr and Hf complexes containing a 1,3-diphosphabicyclo[1.1.0]butanediyl ligand have been found experimentally<sup>[6][7]</sup> (Scheme 3), the cobalt analog CpCo-**5a** has also been calculated. It is found at 256 kJ/mol relative to CpCo-**2a**. Note that CpCo-**5a** was optimized within  $C_s$  symmetry ( $MC_1C_2$  mirror plane). Releasing all symmetry constraints yielded CpCo-**12a**, shown in Figure 4, which still possesses  $C_s$  symmetry, but now with an  $MP_1P_2$  mirror plane. This structure, which has so far not been reported in the literature, possesses a tilted 1,3-diphosphabicyclo[1.1.0]butanediyl ligand, so that a bond between Co and  $P_1$  is formed. Selected geometrical parameters of this molecule are given in Table 5. While the  $C_1P_1$  bond length amounts to 1.951 Å, indicating a single bond, the  $C_1P_2$  distance of 1.811 Å suggests a partial double bond character between the  $C_1$  and  $P_2$  atoms. The folding angle  $C_1P_1P_2C_2$  of 100.4° shows that the 1,3-diphosphabicyclo[1.1.0]butanediyl unit has opened up by about 8° with respect to CpCo-**5a**. The most striking feature of this molecule, however, is its energy. CpCo-**12a** is found at 181 kJ/mol relative to CpCo-**2a** and thus well below the bis( $\pi$ -phosphaalkyne) complexes CpCo-**6a** and CpCo-**7a** (Table 4). Most likely, flattening of the 1,3-diphosphabicyclo[1.1.0]butanediyl unit in CpCo-**12a** uniquely leads to the 1,3-DPCB complex CpCo-**4a**. Therefore, CpCo-**12a** should be regarded as an important candidate for an intermediate in the formation of CpCo-**4a**.

### 3.2.2 Cobalt Complexes of $CH_3-C\equiv P$ Dimers

In order to check the influence of larger R substituents on phosphalkynes, the methyl analogues CpCo-**2b**–CpCo-**11b** have also been calculated (see Figure 2). It is seen from Table 4 that substituting H by  $CH_3$  has a rather moderate effect on the relative energies. The energy gap between the 1,2-DPCB complex CpCo-**2b** and the 1,3-DPCB complex CpCo-**4b** has slightly increased with respect to the hydrogen analogues. The cobalt complexes CpCo-**8b**–CpCo-**11b** are now found at an even higher relative energy than was the

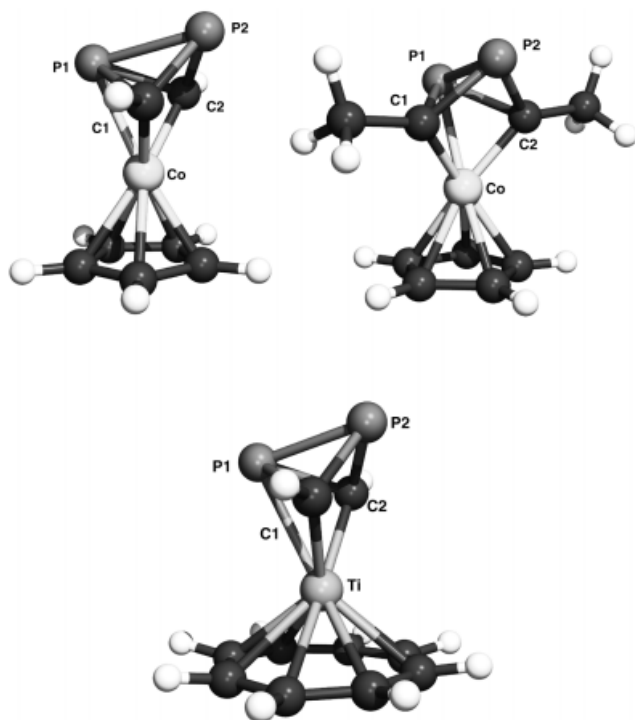


Figure 4. B3LYP-optimized structures of CpCo-12a, CpCo-12b and COT-Ti-12a

Table 5. B3LYP/6-31G(d,p)-optimized bond lengths [Å] and angles [°] of the CpCo-12a, CpCo-12b and COT-Ti-12a structures

	CpCo-12a	CpCo-12b	COT-Ti-12a
MP <sub>1</sub>	2.299	2.299	2.625
MP <sub>2</sub>	2.891	2.877	3.123
MC <sub>1</sub>	1.907	1.908	2.104
C <sub>1</sub> P <sub>1</sub>	1.951	1.964	1.953
C <sub>1</sub> P <sub>2</sub>	1.811	1.818	1.831
C <sub>1</sub> C <sub>2</sub>	2.306	2.335	2.330
P <sub>1</sub> P <sub>2</sub>	2.262	2.262	2.187
C <sub>1</sub> P <sub>1</sub> C <sub>2</sub>	72.4	72.9	73.2
C <sub>1</sub> CoC <sub>2</sub>	74.4	75.5	67.3
C <sub>1</sub> P <sub>1</sub> P <sub>2</sub> C <sub>2</sub>	100.4	101.1	98.2

case for their hydrogen analogues. Hence, in the case of methyl substitution, it is also likely that the proposed reaction mechanism of Scheme 4 is not valid. The complex containing a tilted 1,3-diphosphabicyclo[1.1.0]butanediyl ligand CpCo-12b has also been located and is found at a relative energy of 190 kJ/mol. Hence, similar to the case for R = H, it possibly represents an important intermediate in the formation of DPCB complexes. As CpCo-4b represents the best approximation to the structure of the experimentally known CpCo-4c, some geometrical parameters of the latter have also been included in Table 3. While the calculated metal-phosphorus distances are somewhat longer than the experimental value (by about 0.02 Å), the metal-carbon bond is slightly underestimated by 0.01 Å. The other parameters are in good agreement with experimental values, and the geometry obtained using B3LYP optimization thus seems very reliable.

Since the Cp<sub>2</sub>Zr complex of the 2,4-di-*tert*-butyl-1,3-diphosphabicyclo[1.1.0]butanediyl ligand is known<sup>[6]</sup> (see

Scheme 3), it is also worth comparing the experimental geometry with calculated values for CpCo-5b. Table 3 shows that B3LYP yields good values for the C<sub>1</sub>P<sub>1</sub> and P<sub>1</sub>P<sub>2</sub> distances. The folding angle C<sub>1</sub>P<sub>1</sub>P<sub>2</sub>C<sub>2</sub>, however, is considerably overestimated with respect to the experimental one (93.4° versus 70°). Note, though, that the latter effect could be due to steric interactions of the two Cp ligands with the *t*Bu groups.

### 3.2.3 Titanium Complexes of H-C≡P Dimers

The situation changes quite drastically when COT-Ti is used as the complexing metal fragment (COT = cyclooctatetraene). Only complexes of the HCP molecule have been investigated in conjunction with this metal fragment, since our available computational resources did not allow larger systems to be calculated.

The energy difference between the 1,2-DPCB complex COT-Ti-2a and the 1,3-DPCB complex COT-Ti-4a amounts to 54 kJ/mol, in favor of the former. Both bis(π-phosphaalkyne) complexes COT-Ti-6a and COT-Ti-7a are found at about 270 kJ/mol above COT-Ti-2a.

So far, the situation is quite analogous to the case of cobalt complexes. However, more serious differences appear when turning our attention to the metalla complexes. The complexes COT-Ti-8a and COT-Ti-10a are now lying well below the bis(π-phosphaalkyne) complexes in relative energy. As such, for COT-Ti complexes, these findings support the reaction mechanism shown in Scheme 4. Another important difference – as compared with the cobalt complexes – concerns the COT-Ti-5a species, which contains a 1,3-diphosphabicyclo[1.1.0]butanediyl ligand. While in the case of Co, it was found at relative energies of 250–270 kJ/mol, it is now located at 174 kJ/mol. Hence, COT-Ti-5a is likely to be accessible from the bis(π-phosphaalkyne) complexes, and thus it possibly represents an important intermediate. In analogy to the CpCo-12a complex, containing a tilted 1,3-diphosphabicyclo[1.1.0]butanediyl ligand, COT-Ti-12a has also been located. While its geometry is shown in Figure 4, the corresponding optimized parameters are given in Table 5. Apart, of course, from the MC and MP distances, all values are very similar to the ones derived for CpCo-12a and CpCo-12b. The relative energy of the species COT-Ti-12a is calculated to be 163 kJ/mol with respect to COT-Ti-2a. Hence it is only 11 kJ/mol more stable than its analog containing a non-tilted 1,3-diphosphabicyclo[1.1.0]butanediyl ligand. The species COT-Ti-5a and -12a as well as the metalla complexes COT-Ti-8a–COT-Ti-10a should be considered accessible from the bis(π-phosphaalkyne) complexes. This implies that all of them possibly represent important intermediates in the formation of DPCB complexes. Note that, in the case of Ti complexes, the complex COT-Ti-11a could not be located, in contrast to CpCo-11a and CpCo-11b.

As far as geometry is concerned, both COT-Ti-2c and COT-Ti-4c have been characterized experimentally by X-



ray diffraction.<sup>[11]</sup> Their geometrical parameters are also shown in Table 3. For these species, B3LYP seems to overestimate slightly the metal–phosphorus bond lengths by about 0.02 Å, while the reverse trend is noted for the metal–carbon distances (an underestimation of about 0.05 Å). The most striking discrepancy between experimental and optimized geometries is the fact that, for the 1,3-DPCB complex, B3LYP yields a rhombic C<sub>2</sub>P<sub>2</sub> ligand, having four equal C–P distances, while the experimentally resolved structure shows alternating single and double C–P bonds. At this point, however, it is not clear whether such an inconsistency originates from either a shortcoming of the B3LYP method or an effect of crystal packing or even an electronic effect of the *t*Bu groups.

## 4. Conclusions

In an attempt to tackle some points of controversy and uncertainty concerning the formation and relative stabilities of DPCB complexes, calculations have been carried out on a number of important isomers of [R<sub>2</sub>C<sub>2</sub>P<sub>2</sub>] with R = H, CH<sub>3</sub>, and *t*Bu, [Cp–Co–(R<sub>2</sub>C<sub>2</sub>P<sub>2</sub>)] isomers (R = H, CH<sub>3</sub>; Cp = cyclopentadienyl), and isomers of COT–Ti–[H<sub>2</sub>C<sub>2</sub>P<sub>2</sub>]. Several of these points have been addressed, which lead to new insights into the chemistry of DPCB complexes.

- Concerning the uncomplexed species, the calculations confirm the previous results that the valence isomer of 1,2-DPCB having  $\pi$  bonds between the two C atoms and between the two P atoms tends to be the most stable diphosphacyclobutadiene. The other isomer is found 6 kJ/mol higher in energy for R = H, 10 kJ/mol for R = Me and 16 kJ/mol for R = *t*Bu. The 1,3-DPCB is considerably less stable than 1,2-DPCB for both R = H and Me (53 and 48 kJ/mol, respectively). Only for R = *t*Bu, the 1,2 and 1,3 dimers are found rather close in energy. The fact that the head-to-head dimer turns out to be the most stable, even when large substituents are used, emphasizes its intrinsic stability.

Calculation of the energy barriers for the cycloaddition of two R–C $\equiv$ P molecules, confirms that the head-to-head reaction is not only thermodynamically favored, but also kinetically.

For the parent species (R = H), MP2, and CCSD(T) calculations show that B3LYP yields good results as compared to CCSD(T), whereas the MP2 method is often in considerable deviation with the CCSD(T) level.

- Calculations on the diphosphacyclobutadiene complexes of CpCo show that the relative stability of the head-to-head product versus the head-to-tail product remains almost unchanged as compared to the uncomplexed dimers. In order to check the reaction mechanism proposed in the literature, a number of additional complexes have been calculated, including cobalta species. Due to their high energy content, it is suggested that the 1-cobaltadiphosphacyclopentadiene complexes are unlikely to act as intermediates in the formation of diphosphacyclobutadiene ligands out of bis( $\pi$ -phosphaalkyne) complexes. This observation is in

sharp contrast to the available experimental observations for the all-carbon CpCoCb complexes. However, a rather remarkable and so far unknown species has been located theoretically, containing a tilted 1,3-diphosphabicyclo-[1.1.0]butanediyl ligand. In view of its relative energy, the latter complex is more likely to be an intermediate in the formation of diphosphacyclobutadiene complexes than the cobalta species.

An extension has also been made from R = H to R = Me. Theoretical findings show, however, that substituting H by Me does not affect the conclusions drawn above.

- While the COT–Ti complexes behave rather analogously to the CpCo complexes, one major difference is detected. The metalla ring intermediates, that turn out to be too high in relative energy in the case of CpCo complexes, seem now to be valuable candidates to intervene in the formation of COT–Ti DPCB complexes. As such, in the case of Ti complexes, several routes leading from the bis( $\pi$ -phosphaalkyne) to the diphosphacyclobutadiene complexes seem to be possible. This fact may explain the experimental detection of complexes of both the 1,2- and 1,3-dimers.

A characterization of the complexes considered in this work by harmonic frequency analysis, as well as the location of transition structures connecting the various complexed species, seem thus necessary for a full understanding of the formation of diphosphacyclobutadiene complexes. At this very moment, these calculations are unfortunately quite beyond our computational limits. Nevertheless, we believe that the presented results add several new insights into this interesting problem in low-coordinated phosphorus chemistry.

## Acknowledgments

The authors are indebted to the FWO-Vlaanderen and the GOA program for continuing support.

- [1] P. B. Hitchcock, M. J. Maah, J. F. Nixon, *J. Chem. Soc., Chem. Commun.* **1986**, 737.
- [2] P. Binger, R. Milczarek, R. Mynott, M. Regitz, W. Rösch, *Angew. Chem. Int. Ed. Engl.* **1986**, 25, 644.
- [3] M. Driess, D. Hu, H. Pritzkow, H. Schäufele, U. Zennek, M. Regitz, W. Rösch, *J. Organomet. Chem.* **1987**, 334, C35.
- [4] P. Binger, B. Biedenbach, R. Schneider, M. Regitz, *Synthesis* **1989**, 960.
- [5] T. Wettling, G. Wolmershäuser, P. Binger, M. Regitz, *J. Chem. Soc., Chem. Commun.* **1990**, 1541.
- [6] P. Binger, B. Biedenbach, C. Krüger, M. Regitz, *Angew. Chem.* **1987**, 99, 798.
- [7] T. Wettling, B. Geissler, R. Schneider, S. Barth, P. Binger, M. Regitz, *Angew. Chem.* **1992**, 104, 761.
- [8] K. Jonas, *Angew. Chem.* **1985**, 97, 292.
- [9] K. P. C. Vollhardt, *Angew. Chem.* **1984**, 96, 525.
- [10] P. Binger, B. Biedenbach, R. Mynott, C. Krüger, P. Betz, M. Regitz, *Angew. Chem.* **1988**, 100, 1219.
- [11] P. Binger, G. Glaser, S. Albus, C. Krüger, *Chem. Ber.* **1995**, 128, 1261.
- [12] P. Binger, G. Glaser, J. Stannek, *Phosphorus Sulfur Silicon* **1996**, 109–110, 149.
- [13] T. Wettling, J. Schneider, O. Wagner, C. Kreiter, M. Regitz, *Angew. Chem. Int. Ed. Engl.* **1989**, 28, 1013.
- [14] M. T. Nguyen, L. Landuyt, L. G. Vanquickenborne, *J. Org. Chem.* **1993**, 58, 2817.



- [15] A. D. Becke, *J. Chem. Phys.* **1993**, *98*, 5648.
- [16] C. Lee, W. Yang, R. G. Parr, *Phys. Rev. B* **1988**, *37*, 785.
- [17] A. Schäfer, H. Horn, R. Ahlrichs, *J. Chem. Phys.* **1992**, *97*, 2571.
- [18] A. J. H. Wachters, *J. Chem. Phys.* **1970**, *52*, 1033.
- [19] P. J. Hay, *J. Chem. Phys.* **1977**, *66*, 4377.
- [20] M. J. Frisch, G. W. Trucks, H. B. Schlegel, G. E. Scuseria, M. A. Robb, J. R. Cheeseman, V. G. Zakrzewski, J. A. Montgomery, Jr.; R. E. Stratmann, J. C. Burant, S. Dapprich, J. M. Millam, A. D. Daniels, K. N. Kudin, M. C. Strain, O. Farkas, J. Tomasi, V. Barone, M. Cossi, R. Cammi, B. Mennucci, Pomelli, O.; C. Adamo, S. Clifford, J. Ochterski, G. A. Petersson, P. Y. Ayala, Q. Cui, K. Morokuma, D. K. Malick, A. D. Rabuck, K. Raghavachari, J. B. Foresman, J. Cioslowski, J. V. Ortiz, B. B. Stefanov, G. Liu, A. Liashenko, P. Piskorz, I. Komaromi, R. Gomperts, R. L. Martin, D. J. Fox, T. Keith, M. A. Al-Laham, C. Y. Peng, A. Nanayakkara, C. Gonzalez, M. Challacombe, P. M. W. Gill, B. Johnson, W. Chen, M. W. Wong, J. L. Andres, C. Gonzalez, Head-M. Gordon, E. S. Replogle, J. A. Pople, *GAUSSIAN 98, Rev. A.5*, Gaussian Inc., Pittsburgh PA, **1998**.
- [21] IBM Research Division, Chemical Services and Applications, Almaden Research Center, 650 Harry Road San Jose, CA 95120–6099, USA, *Mulliken, version 1.1.0*, **1994**.
- [22] P. Binger, R. Milczarek, R. Mynott, C. Krüger, Y.-H. Tsay, E. Raabe, M. Regitz, *Chem. Ber.* **1987**, *121*, 637.
- [23] G. A. Ville, K. P. C. Vollhardt, M. J. Winter, *Organometallics* **1984**, *3*, 1177.

Received October 20, 1998  
[198361]